

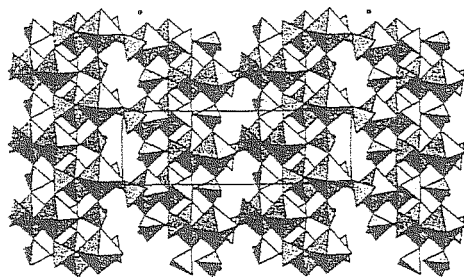
and their dependence on such synthetic parameters as pH, sulfur content, temperature and aging, the transformations from starting materials. We have done this under real-time hydrothermal conditions using powder diffraction and an IP at beamline X7B. From these results, information on the kinetics of formation, useful to optimize future syntheses, has been obtained.

**PS10.10.13 THE SYNTHESIS AND CRYSTAL STRUCTURES OF ALKALINE EARTH METAL INDIUM PHOSPHATES.** Xuejiao Tang and Abdessadek Lachgar, Chemistry Department, Wake Forest University, Winston-Salem, NC 27109-7486.

Metal phosphates with open framework structures are well known for their adsorptive, catalytic and ion-exchange properties. Al and Ga phosphates have been widely studied and exhibit great structural variations. In contrast, research of In phosphates has been very limited in scope. As a part of our search for open framework metal phosphates, we have recently been investigating ternary alkali or alkaline earth metal indium phosphates using hydrothermal synthesis techniques.

We report the syntheses and crystal structures of alkaline earth metal indium phosphates  $A[\text{In}_2(\text{PO}_4)_2(\text{HPO}_4)]$  ( $A=\text{Ca}$ ,  $\text{Sr}$  or  $\text{Ba}$ ).  $\text{Ca}[\text{In}_2(\text{PO}_4)_2(\text{HPO}_4)]$  was synthesized hydrothermally from stoichiometric amounts of  $\text{CaO}$  and  $\text{InCl}_3$  in excess  $\text{H}_3\text{PO}_4$  and  $\text{H}_2\text{O}$ . The compound crystallizes in monoclinic symmetry, space group  $P2_1/n$ ,  $a=6.5708(6)$ ,  $b=20.237(2)$ ,  $c=6.6572(7)\text{\AA}$ ,  $\beta=91.20(1)^\circ$ . The structure contains  $\text{In}_2\text{O}_{10}$  dimers built up of two edge-sharing ( $\text{InO}_6$ ) octahedra. The dimers connect to each other through ( $\text{PO}_4$  or  $\text{HPO}_4$ ) tetrahedra by sharing all of their oxo ligands. Cations are located in tunnels of 8-member ring opening running along [001] direction. To our knowledge, this is the first reported indium phosphate containing  $\text{In}_2\text{O}_{10}$  dimers.

$\text{Sr}[\text{In}_2(\text{PO}_4)_2(\text{HPO}_4)]$  was obtained hydrothermally from  $\text{Sr}(\text{OH})_2$  and  $\text{InCl}_3$  (1:1) in excess  $\text{H}_3\text{PO}_4$  and  $\text{H}_2\text{O}$ . Space group  $P2_1/n$ ,  $a=6.615(1)$ ,  $b=20.351(3)$ ,  $c=6.752(1)\text{\AA}$ ,  $\beta=91.00(1)^\circ$ . Its structure is analogue to  $\text{Ca}[\text{In}_2(\text{PO}_4)_2(\text{HPO}_4)]$



**PS10.10.14 ORIENTATION OF NAPHTHALENE IN H-ZSM-5 AS DETERMINED FROM POWDER AND SINGLE CRYSTAL XRAY DATA.** H. van Koningsveld and J. C. Jansen, Labs. of Applied Physics and Organic Chemistry and Catalysis, Delft University of Technology, Lorentzweg 1, 2628 CJ Delft, The Netherlands

The adsorption properties of frameworks with the MFI topology (H-ZSM-5 and its Al-free analogue silicalite-1) have received much attention. There is a general agreement that in low-loaded MFI/adsorbent systems the preferred adsorption site is at the intersection of channels.

Recently published papers on the localization of naphthalene (nph) in H-ZSM-5 determined by X-ray Powder Diffraction (hereafter referred to as XPD1 [Mentzen et al.; Zeolites, 13 (1993) 485] and XPD2 [Klein et al.; Microporous Materials, 3 (1994) 291]) show inconsistent results.

In both papers the structure is described in the orthorhombic space group  $Pnma$ . In XPD1 as well as in XPD2 the nph molecules (3.8 and 3.0

mol/u.c., respectively) are at the intersection of channels. However, the inversion of the unit cell axes  $a$  and  $b$  ( $a/b < 1$ ; the empty orthorhombic HZSM-5 framework has  $a/b > 1$ ), as observed in XPD1, is not reported in XPD2. In addition, the orientation of the nph molecules at the intersection of channels in XPD1 and XPD2 is quite different.

We succeeded in preparing a single crystal of the H-ZSM-5 zeolite loaded with 3.68(2) molecules nph per u.c., large enough to allow a single crystal X-ray diffraction study of the material.

The paper describes the structure of the H-ZSM-5/nph complex, gives the ensuing deformation of the channel pores and compares the orientation of nph as determined from powder and single crystal X-ray diffraction. The inversion of the  $a$  and  $b$  axes is confirmed and the orientation of nph is yet different from the orientations reported in the XPD-papers.

**Materials XI  
Fullerenes**

**MS10.11.01 DETERMINATION OF THE ENDOHEDRAL NATURE OF THE METALLOFULLERENE  $\text{Y}@\text{C}_{82}$  BY MEM.** M. Takata, E. Nishibori, B. Umeda, M. Sakata, M. Ohno, H. Shinohara & Y. Saito\*, Nagoya University, Nagoya 464-01, Japan, \*Mie University, Tsu 514 Japan

The first conclusive evidence of endohedral nature of the Metallofullerene  $\text{Y}@\text{C}_{82}$  has been obtained via a Synchrotron X-ray powder diffraction study using the Maximum Entropy Method (MEM). Recently, the synthesis of fullerenes encapsulating various metal atoms within the carbon cage (endohedral metallofullerenes) has stimulated wide interest because of their unusual structural and electronic properties. Observations using STM, EXAFS, HRTEM and ESR have strongly suggested that the metal atoms are indeed inside the fullerene cage. Theoretical calculations also indicate that this is the case. But until now, no structural model has been derived experimentally to confirm the endohedral nature of the metallofullerenes. The  $\text{Y}@\text{C}_{82}$  fullerene was separated and isolated by the two-stage high performance liquid chromatography (HPLC) method. The purity of the  $\text{Y}@\text{C}_{82}$  fullerene was more than 99.9%. An X-ray powder pattern of  $\text{Y}@\text{C}_{82}$  was measured by using Imaging Plate at Photon Factory BL-6A2. The wavelength of incident X-rays is  $1.0\text{\AA}$ . The space group is assigned to  $P2_1$ , monoclinic. The experimental data were analyzed in an iterative way of combination of Rietveld analysis and the MEM. The reliable factor of the obtained MEM charge density is 1.4%. In the MEM charge density, there exist remarkably high densities just inside the  $\text{C}_{82}$  cage. The number of electrons around the maxima is about 38 which is very close to the atomic number of a yttrium atom. Evidently, the density maxima at the interior of the  $\text{C}_{82}$  cage is the yttrium atom. The present study revealed the fact that the yttrium atom is displaced from the centre of the  $\text{C}_{82}$  molecule and is strongly bound to the carbon cage.

**MS10.11.02 X-RAY DIFFUSE SCATTERING AND INTER-MOLECULAR INTERACTIONS IN SOLID  $\text{C}_{60}$ .** R. Moret, P. Launois and S. Ravy, Laboratoire de Physique des Solides, URA CNRS 02, Université Paris-Sud, 91405 Orsay, France

Orientalional ordering phenomena control the temperature-pressure phase diagram of solid  $\text{C}_{60}$ . At present, their understanding is imperfect because microscopic models fail to describe the interactions between the fullerene molecules in details.

Above the  $T_0=259\text{K}$  orientational ordering transition the molecules do not rotate freely in the cubic crystal-field and significant short-range orientational correlations are present. They produce radial and azimuthal modulations of the diffuse scattering intensity which have been measured carefully in the first halo ( $Q \approx 3.3\text{\AA}^{-1}$ ) by single crystal X-ray diffraction. Intensity maxima at the special points  $X(100)$ ,  $L(1/2, 1/2, 1/2)$  and  $\Gamma(000)$  of the Brillouin zone together with some "extra" scattering have been

identified<sup>1</sup>. The X-point maxima can be considered as precursor effects of the low temperature Pa  $\bar{3}$  phase, while the other diffuse scatterings may reveal the existence of competing phases. By comparing the observed intensity distribution to that calculated using a microscopic mean-field theory (with the formalism of the symmetry adapted functions, up to the  $l=12$  terms) we evaluate different models of intermolecular potential. Van der Waals-type intermolecular interactions are found to account for the main features of the observed diffuse scattering<sup>2</sup>. Elaborate models of intermolecular potential are being tested.

Below  $T_0$ , the remaining X-ray diffuse scattering is analyzed to clarify the orientational order of the nearly degenerate configurations of the  $C_{60}$  molecules ("penta" and "hexa") which coexist in the Pa  $\bar{3}$  phase.

<sup>1</sup> P. Launois, S. Ravy and R. Moret, Phys. Rev. B52, 5414 (1995).

<sup>2</sup> S. Ravy, P. Launois and R. Moret, submitted.

**MS10.11.03 GEOMETRY AND STABILITY OF GRAPHITIC ONION-LIKE STRUCTURES.** Terrones, H., Instituto de Fisica UNAM, Apartado, Postal 20-364, C.P. 01000, Mexico, D.F. and Terrones M., School of Chemistry and Molecular Sciences, University of Sussex, Brighton BN1 9QJ, U.K

Using energy minimization with heptagonal and pentagonal rings of carbon in a graphite hexagonal mesh, we have produced quasi-spherical giant fullerenes which are suitable for forming stable bucky onions. A formation mechanism which explains the transformation, during high electron irradiation, of polyhedral graphite particles into graphitic onions is proposed. According to our mechanism, the most strained parts of the polyhedral particles (pentagonal rings and adjacent atoms) are destroyed during the irradiation generating flexible holey structures which can be moulded by energy minimization to obtain quasi-spherical giant fullerenes with holes. The holes are filled with heptagonal and pentagonal rings preserving the sphericity and avoiding the faceting characteristic of giant fullerenes with just 12 pentagonal rings. We also show that bucky-onions can be ordered (symmetric) or amorphous (non-symmetric) on the surface of a sphere. In general, the role of defects such as pentagons, heptagons and octagons in fullerenes, nanotubes and negatively curved graphite is analyzed. All these new structures open the field of a generalized crystallography in which atoms rest on surfaces with different curvatures: zero Gaussian curvature for nanotubes, positive curvature for fullerenes and negative curvature for cork-screw nanotubes and other hypothetical arrangements waiting to be discovered.

**MS10.11.04 NEW STRUCTURAL STUDIES OF CHEMICALLY MODIFIED FULLERENES.** Alan L. Balch, Marilyn M. Olmstead, David A. Costa, Arwa Ginwalla, David Lane, Department of Chemistry, University of California, Davis, CA 95616.

Recent results of structural work on chemically modified fullerenes that bear organometallic or organic functionalities covalently bonded to the fullerene surface will be described. Emphasis will be placed on the characterization of fullerene oxides and oxidation products (i.e.  $C_{70}O$ ) and on addition products where Vaska's Compound,  $Ir(CO)Cl(PR_3)_2$ , is used to prepare suitable crystalline samples.

**MS10.11.05 MOMENTUM DENSITY OF  $K_xC_{60}$ .** G. Loupías, Ch. Bellin, M. Marangolo, J. Moscovici, S. Erwin, S. Rabii, C. Hérold, J.F. Maréché, P. Lagrange. Université Pierre et Marie Curie (Paris 6), 4, place Jussieu 75252 Paris Cedex 05.

Compton scattering measurements have been demonstrated to provide an accurate check of valence electron densities of solids, in the electronic ground-state. Since the scattering is incoherent, this technique, which is a bulk probe, is insensitive to crystal defects.

Compton profiles, i.e. energy-loss spectra of scattered photons were measured on powder samples, using 16keV monochromatic beam provided by the french synchrotron facility. All the  $K_xC_{60}$  samples ( $x=3,4$ , and 6) were intercalated by C. Hérold *et al.* and kept under vacuum. For comparison,  $C_{60}$  powder was measured in same experimental conditions. Average calculated Compton profiles are simulated by S. Rabii from the *ab initio* and all-electron SCF energy band structure calculated by S. Erwin within the local-density approximation (LDA).

In order to describe the electronic structures, differences between  $K_xC_{60}$  and  $C_{60}$  measured Compton profiles are compared with theoretical profile differences. Since Compton scattering is particularly sensitive to the hybridization between carbon and alkali orbitals as it was demonstrated in the case of graphite intercalation compounds, the distortion of  $C_{60}$  molecule is discussed as a function of  $x$ . In addition, "charge transfer" between the intercalate and the  $C_{60}$  molecules as well as magnitude of e-e- correlations (essential to understand the superconductivity) are studied in this set of materials.

[1] Loupías G. and Petiau J., *J. Physique* **41** (1980) 265-271

Loupías G., Petiau J., A. Issolah, Schneider M., *Phys. Stat. Sol. B*, **102** (1980) 79-89.

[2] Erwin S. C., *Buckminsterfullerenes*, Billups W. E. and Ciufolini M. A., Eds., VCH Publishers, New York, (1993) 217

Erwin S. C. and Pederson M. R., *Phys. Rev. Lett.*, **67** (1991) 1610.

[3] Rabii S., Chomilier J., Loupías G., *Phys. Rev* **B40**, (1989) 10 105.

[4] Chou M. Y., Lam P. K., Marvin L. Cohen, Loupías G., Chomilier J., and Petiau J., *Phys. Rev. Letters*, **19** (1982) 1452.

**MS10.11.06 PHASES IN THE  $A_1C_{60}$  SYSTEM (A=K, Rb, Cs).** G. Faigel, G. Bortel, L. Gránásky, G. Oszlányi, S. Pekker, T. Pusztai, M. Tegze, Research Institute for Solid State Physics, H-1525 Budapest, POB. 49., Hungary; L. Forró, IGA, Ecole Polytechnique Federale de Lausanne, 1015 Lausanne, Switzerland; P.W. Stephens, G. Bendele, Department of Physics, SUNY, Stony Brook, NY 11794, USA.

The crystalline structure of the various phases of  $A_1C_{60}$  type salts (A=K, Rb, Cs) were determined from x-ray powder diffraction.

In the short time since the discovery of  $C_{60}$ , an amazing variety of compounds have been found. In most of them the intermolecular separation is mainly determined by van der Waals interactions. Recently some exceptions have been found, in which  $C_{60}$  molecules are linked by covalent bonds. Among them the orthorhombic phase of  $A_1C_{60}$  was the first for which x-ray diffraction clearly proved the existence of linear polymer chains. In all cases the basic mechanism of polymerization is [2+2] cycloaddition which involves hexagon-hexagon bonds of neighbouring  $C_{60}$  molecules.

Polymer formation in  $A_1C_{60}$  can be prevented by fast cooling from high temperature. In this case covalent  $(C_{60})_2$  dimers are formed through a single C-C bond which differs from the bonding configuration of the polymer.

The sequence of phase transitions between the various phases was successfully modelled by a parameter free Monte Carlo type calculation giving a microscopic picture of these processes.

An inhomogeneous structural phase specific to  $K_1C_{60}$  appears at 400 K. In this "intermediate state" the K ions are distributed in such a way that small  $K_3C_{60}$  and K free  $C_{60}$  regions are formed while the  $C_{60}$  sublattice remains continuous. The structure has important consequences on the physical properties.